THE JOURNAL OF PHYSICAL CHEMISTRY C

Article

pubs.acs.org/JPCC

All-Optical Nanometric Switch Based on the Directional Scattering of Semiconductor Nanoparticles

Braulio García-Cámara,*[,†] J. Francisco Algorri,[†] Alexander Cuadrado,[‡] Virginia Urruchi,[†] José Manuel Sánchez-Pena,[†] Rosalía Serna,[‡] and Ricardo Vergaz[†]

[†]Group of Displays and Photonic Applications (GDAF-UC3M), Electronic Technology Department, Carlos III University of Madrid, Avda. de la Universidad n° 30, 28911, Leganés, Madrid, Spain

[‡]Laser Processing Group, Instituto de Óptica, CSIC, C/Serrano 121, 28006, Madrid, Spain

ABSTRACT: A structure based on a dimer of silicon nanoparticles, presenting directional scattering in the visible range, was studied as a new design of an all-optical switch. The combination of spherical nanoparticles satisfying, at the same incident wavelength, the zero-backward and the minimum-forward scattering conditions can produce either a maximum or a minimum of the scattered field in the area between the nanoparticles. The modulation of the incident wavelength can be used as a switching parameter due to the sensitivity of these conditions to it. An optimization of the dimer setup, both in the distance between the nanoparticles and the incident wavelength, was numerically performed to obtain a maximum contrast. Also, near-field and far-field distributions of the electric field have been considered.

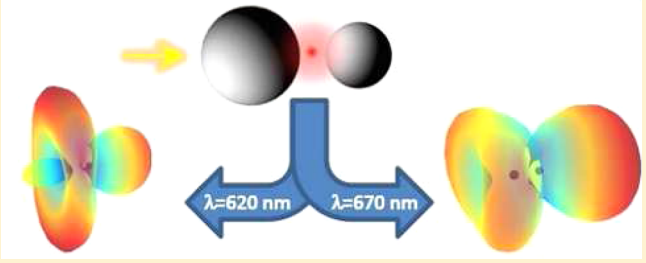

INTRODUCTION

Since the famous lecture of Richard P. Feynman,[1] so far, the understanding and control of the physics in the nanoscale have not stopped. In fact, this work is focused on one of these recent discoverings, in particular, the directionality of light scattering of magnetodielectric nanoparticles, like silicon nanoparticles, and its use in new photonic devices. Until now, in photonics, the control and manipulation of light at subwavelength dimensions has been the main challenge. Fortunately, nowadays, this is possible thanks to the interaction between light and nanoscale structures. Consequently, photonics is now present in a large amount of applications in the nanometric range, from the design of novel and high sensitive nanobiosensors[2] to photonic on-chip devices.[3] In this latter case, photonic devices are being proposed as efficient optical counterparts of current electronic devices.[4,5] Several functionalities, such as information storage,[6] switching,[7] communications,[8,9] or even the manipulation of information,[10,11] have been explored using photonic nanotools. However, the weak interaction between light and nanometric devices requires the presence of resonant systems to obtain measurable signals. Light resonances in metallic nanostructures, known as plasmon resonances, are one of the main physical phenomena used for the control and manipulation of light at the nanoscale. The collective oscillation of the free electrons on the surface of the metal produces a strong enhancement of both the scattering and absorption of light.[12] These effects are now present in a wide range of applications and devices in such diverse fields, from the visible to the terahertz range.[13] Different sensors,[14−16] subdiffraction limit imaging,[17] or nanoantennas[18,19] are some examples of a myriad of them. The use of plasmonic materials has an important disadvantage for several applications: the ohmic losses. For this reason, the interest on resonant dielectric nanostructures arose in the last years because of the interesting properties of dielectric nanoparticles with high refractive index (e.g., silicon, Germanium, etc.). They are low-losses, present light resonances, and they are CMOS compatible. In addition, these nanoparticles are able to respond to both the electric and the magnetic part of electromagnetic waves.[20,21] These effects make that resonant dielectric nanoparticles can be not only an ideal counterpart of plasmonic nanoparticles, they may be also the basis of new devices using the magnetic properties of the nanoparticles. In this sense, a great number of new applications have arisen in the last years employing dielectric nanostructures.[22]

Some previous applications are based on either simple or complex arrangements of these nanosystems. Metamaterials are probably the most impressive application of an arrangement of resonant nanoparticles. These complex media allow obtaining desired optical properties, which do not exist in nature, and they have only been observed employing metamaterials. Epsilon-near-zero (ENZ), epsilon-very-large (EVL), artificial magnetics, or left-handed (LH) media are developed using metamaterials.[23−25] Nanoantennas and oligomers are more simple arrangements of resonant nanoparticles, but with important applications as well. For instance, nanoantennas, which were first considered as signal sources, are currently used for other interesting applications, such as near-field microscopy,

Received: July 1, 2015
Revised: July 27, 2015
Published: July 31, 2015

DOI: 10.1021/acs.jpcc.5b06302
J. Phys. Chem. C 2015, 119, 19558−19564

biomedical sensors, or high-efficiency photovoltaics.[26] In addition, the use of resonant dielectric nanoparticles allows the introduction of the concept of superdirective nano-antennas.[27] On the other hand, oligomers are symmetrically positioned nanoparticles, which interest lies on the excitation of Fano resonances.[28] The extreme sensitivity of this kind of resonances with the optical properties of the environment makes them very useful for sensing.[29] Again, oligomers of dielectric nanoparticles also present Fano resonances.[30−33] Even the simplest arrangement of nanoparticles, a dimer, has been already analyzed for different applications. For instance, considering semiconductor nanoparticles, the presence of both electric and magnetic resonances has been used to produce both electric and magnetic hotspots[34,35] for spectroscopic techniques.[36]

Also, there is an interaction between the electric and the magnetic modes that a single dielectric nanoparticle can support. This interaction presents coherent effects producing directional scattering, as it is stated in studies made by Kerker and co-workers more than 30 years ago.[37,21,38] In this work, we study the possibility to design an all-optical switch based on this effect. In fact, we analyze the interaction between two semiconductor nanoparticles forming a simple dimer, including also the influence of these other interferential effects, the directional conditions. In particular, we consider a dimer of silicon (Si) nanoparticles with different sizes in such a way that one satisfies the first Kerker's condition, or the zero-backward scattering condition, and the other one satisfies the second Kerker's condition, or the minimum-forward scattering condition, at the same incident wavelength. Optimizing different parameters, like the distance between the nanoparticles, we will be able to produce either a maximum (hotspot) or a minimum of light in the region between both nanoparticles. Due to the small scattering cross section of both nanoparticles at Kerker's conditions, the signal at the interparticle region is not so high, frustrating its use in applications based on a field enhancement.[35] However, a slight shift of the incident wavelength produces a failing of Kerker's conditions and a strong change of the light concentration in this area. We propose that this sensitivity can be used to obtain "bright" or "dark" points from a dynamical point of view, and it can be the base to develop an all-optical switch in which two different states correspond to the fulfilling or not of Kerker's conditions.

THEORETICAL BACKGROUND

The interaction of light with spherical particles is usually described by the capacity of the particle to remove electromagnetic energy from the incident beam by scattering and absorption effects. Mie theory offers a simple way to depict these effects from an analytical point of view, using a multipolar decomposition.[39] Considering a homogeneous and isotropic spherical particle with a radius R that is illuminated by a linearly polarized plane wave with a wavelength λ, its extinction (scattering + absorption, C_{ext}), scattering (C_{sca}), and absorption (C_{abs}) cross sections are given by

$$C_{ext} = \frac{2\pi}{k^2}\sum_{n=1}^{\infty}(2n+1)\mathrm{Re}\{a_n + b_n\}$$
$$C_{sca} = \frac{2\pi}{k^2}\sum_{n=1}^{\infty}(2n+1)(|a_n|^2 + |b_n|^2)$$
$$C_{abs} = C_{ext} - C_{sca} \quad (1)$$

where k is the wavenumber of the incident beam ($k = 2\pi/\lambda$) and a_n and b_n are the multipolar Mie coefficients that are also known as scattering coefficients. Although these parameters provide complete information, it is usual to use the dimensionless efficiencies, which are defined as

$$Q_{ext} = \frac{2}{x^2}\sum_{n=1}^{\infty}(2n+1)\mathrm{Re}\{a_n + b_n\}$$
$$Q_{sca} = \frac{2}{x^2}\sum_{n=1}^{\infty}(2n+1)(|a_n|^2 + |b_n|^2)$$
$$Q_{abs} = Q_{ext} - Q_{sca} \quad (2)$$

These efficiencies are the result of dividing the corresponding cross sections by the particle cross sectional area projected onto a plane perpendicular to the incident beam. In the case of a spherical particle of radius R, this area is given by $\pi \cdot R^2$. The size parameter (x) is defined as $x = k \cdot R$. This nomenclature leads to a treatment of the electromagnetic field where its multipolar character arises. In particular, a_n coefficients are usually associated with the electric behavior, while b_n coefficients corresponds to the magnetic one. Additionally, first order coefficients (a_1, b_1) are related to the dipolar character, both electric and magnetic, while second order coefficients refer to the quadrupolar phenomena, and so on.

The interest in directional scattering of a nanostructure involves the ability to optimize the differential scattering efficiencies in certain directions. In particular, the scattering in the forward and the backward directions are depicted by the forward scattering (Q_{FS}) and radar backscattering (Q_{RBS}) efficiencies, respectively:[39]

$$Q_{FS} = \frac{1}{x^2}\left|\sum_{n=1}^{\infty}(2n+1)(a_n + b_n)\right|^2$$
$$Q_{RBS} = \frac{1}{x^2}\left|\sum_{n=1}^{\infty}(2n+1)(-1)^n(a_n - b_n)\right|^2 \quad (5)$$

For the case of subwavelentgh particles ($R/\lambda \ll 1$), the light interaction can be described by the first two Mie coefficients (a_1 and b_1) with a negligible loss of information. Considering these conditions, Kerker and co-workers[37] were the first to report that small particles can present a lack of scattering in the forward or the backward directions under certain conditions of the scattering coefficients. These conditions, known as zero-forward and zero-backward conditions or Kerker's conditions, are, respectively:

$$\mathrm{Re}(a_1) = -\mathrm{Re}(b_1);\quad \mathrm{Im}(a_1) = \mathrm{Im}(b_1)$$
$$a_1 = b_1 \quad (6)$$

DOI: 10.1021/acs.jpcc.5b06302
J. Phys. Chem. C 2015, 119, 19558−19564

RESULTS AND DISCUSSION

From a previous work,[40] we can predict that a Si sphere, which is illuminated by a plane wave linearly polarized and with a wavelength of 700 nm satisfies the zero-backward scattering condition when its radius is 82 nm. On the other hand, it fulfills the second Kerker's condition or the minimum-forward scattering condition, when its radius is 96 nm. Figure 1

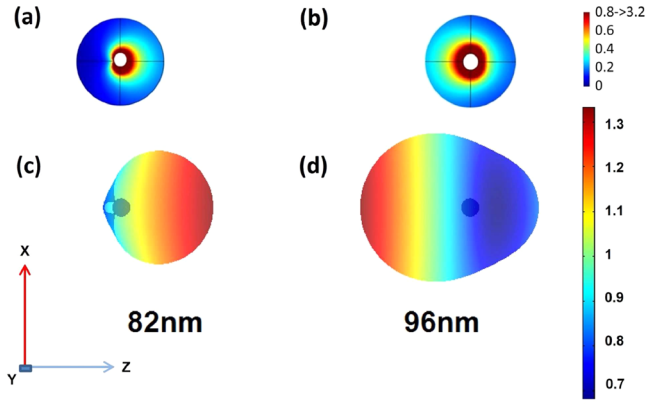

Figure 1. Scattered field in the near-field (upper panel) and the far-field (bottom panel) of a silicon particle with a radius of 82 nm (a, c) and 96 nm (b, d) such that the zero-backward and the minimum-forward conditions are fulfilled, respectively. The incident beam is a plane wave with a wavelength of 700 nm and it is linearly polarized in the parallel direction (x-axis). Scales are normalized to incident field.

shows the scattered field in the near field (a, b) and the far field (c, d) regions of these two silicon nanoparticles, satisfying the directional conditions, eq 6. The incident beam propagates along the positive z-axis and it is linearly polarized parallel (x-axis) to the scattering plane. However, a perpendicular polarization produces similar results due to the spherical symmetry of the system. These results were obtained through FEM simulations (Comsol Multiphysics). It can be seen that an almost null backscattering can be obtained in the zero-backscattering condition, while the forward scattering is only reduced at the zero-forward one, but it cannot be suppressed. It can be also observed that although the asymmetry of light scattering is observed in the near-field region, it is more pronounced in the far-field. The incident wavelength has been chosen arbitrarily. The problem can be easily shifted to other wavelengths considering appropriate particles sizes. The linear dependence of the wavelengths at which directional conditions appears as a function of the particle size[40,41] makes easy to find pairs of particle sizes fulfilling Kerker's conditions for each wavelength.

We guess that a dimer composed of two of these particles can use their asymmetric scattering to produce high or low concentration of the scattered field in the region between them, using them as switching states of an optical device. In particular, we consider a geometrical system as that described in Figure 2a. It is composed of two nanoparticles made of silicon, with different sizes (R_1 and R_2) that are aligned and separated a distance d. The set is illuminated by a monochromatic plane wave that is linearly polarized, either parallel or perpendicular to the scattering plane, impinging from left to right. The sizes of the particles are those considered previously: R_1 = 96 nm and R_2 = 82 nm. This means that the particle on the left mainly scatters in the backward direction, while the other one mainly scatters in the forward direction. Under this configuration, we

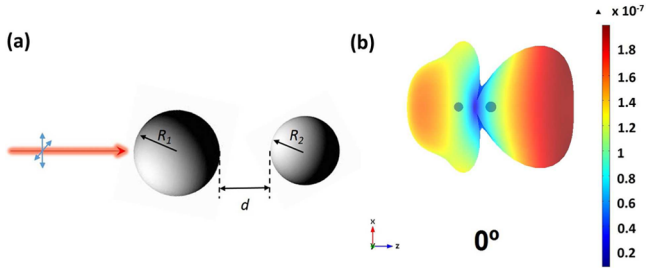

Figure 2. (a) Scheme of the considered dimer. It is composed of two spherical Silicon nanoparticles, with different size (R_1 and R_2), that are aligned, separated a certain distance (d) and illuminated by a plane wave linearly polarized, either parallel or perpendicular to the scattering plane with a wavelength of 700 nm. The arrangement and illumination is such that the directional scattering of the particles are focused on the contrary direction to the gap between them. (b) Spatial distribution of the scattered field of the dimer in the far-field region when the distance between the particles (gap distance) is d = 400 nm.

expect to obtain a minimum light scattering in the gap between the particles.

Figure 2b shows the scattered field of the dimer of the two considered silicon nanoparticles (dark spheres) separated a distance of 400 nm and illuminated with a plane wave of 700 nm linearly polarized parallel to the scattering plane (x-axis) and propagating from the left to the right (z-axis), obtained by FEM simulation. As it was expected a minimum of the scattered field is found in the gap region between the nanoparticles. On the other hand, if the arrangement of the system is the inverted one, such that both nanoparticles mainly scatter into the gap region, a maximum electromagnetic field is expected in this area. Figure 3 shows these results using a FEM simulation. A

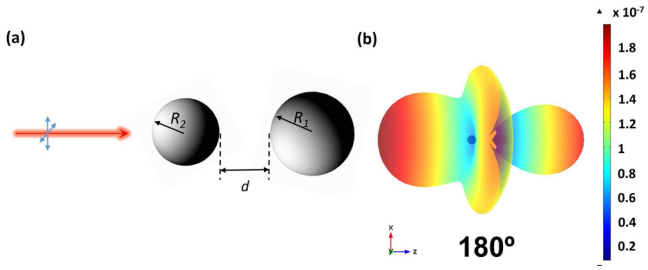

Figure 3. (a) Scheme of the reversed dimer. It is composed of two spherical silicon nanoparticles, with different size (R_2 and R_1), that are aligned, separated a certain distance (d) and illuminated by a plane wave linearly polarized, either parallel or perpendicular to the scattering plane,with a wavelength of 700 nm. The arrangement and illumination is such that the directional scattering of the particles are focused on the gap between them. (b) Spatial distribution of the scattered field of the dimer in the far-field region when the distance between the particles (gap distance) is d = 400 nm.

clear difference between these two arrangements is observed, in particular in the gap region (see Figures 2b and 3b), where the electric field intensity changes drastically.

Both the maximum and the minimum scattered field intensity in the gap region can be optimized by means of a convenient gap distance. In this case, the coherent effects between the electric and the magnetic dipoles present in both particles and producing the zero-backward and the minimum forward scattering join to an interferential effect of the fields in this area. Using an iterative process, the distance producing a constructive or destructive interference can be obtained. In

DOI: 10.1021/acs.jpcc.5b06302
J. Phys. Chem. C 2015, 119, 19558−19564

Figure 4, we show the total (a, b) and the scattered (c, d) electric field in the middle point between the nanoparticles as a

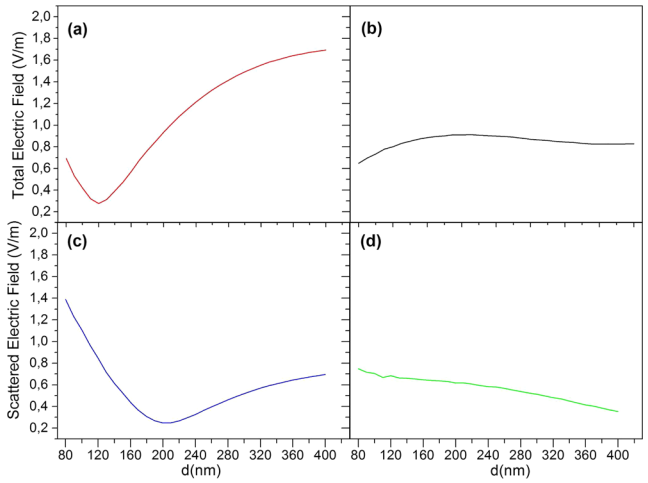

Figure 4. Total (upper panel) and scattered (bottom panel) electric field in the middle point of the gap between the two nanoparticles of Figure 2 as a function of the gap distance (d) between them and with an incident beam with λ = 700 nm. Left: light impinges at 180°, as in Figure 3a configuration. Right: arrangement of Figure 2a.

function of the gap distance (d) between them when the incident field has a wavelength of 700 nm. While the right panel corresponds to the arrangement producing a minimum in the gap region (Figure 2a), the left one corresponds to the arrangement producing a maximum (Figure 3a). An experimental measurement of the scattered field is not a trivial task, and for this reason we also considered the total field, including the influence of both the scattered and the incident field.

The configuration of Figure 3a, producing maximum field intensity in the gap region, presents a remarkable destructive interference effect (see minima at Figure 4a,c). On the contrary, the configuration of Figure 2a is such that the directional effect is dominant. In this work we focus on this configuration, searching for the optimum distance (d = 360 nm according to Figure 4b). Further research will be done for the interference effects on the other configuration.

Focused in the optimum configuration found above, that is, the arrangement of nanoparticles producing a minimum in the gap region and separated a distance of d = 360 nm, we explore the variation of both the scattered and the total electric field in the gap region as a function of the incident wavelength. This search is motivated by the well-known dependence on the wavelength of Kerker's conditions,[37] in particular, for the minimum-forward scattering condition. This dependence is clearly observed in Figure 5. In this case, we plot both the total (Figure 5a) and the scattered electric field (Figure 5b) in the middle point of the gap region of the considered structure as a function of the incident wavelength. In both cases, a local and a global minimum are observed, as well as two remarkable maxima. The main minimum corresponds to the wavelength at which both Kerker's conditions are satisfied. Out of this wavelength, the behavior of the dimer is different from the one that we required. This is also shown in Figure 6a–e, where the far-field distribution of the scattered electric field at certain wavelengths around the minimum is plotted. These wavelengths are highlighted in Figure 5 with circles.

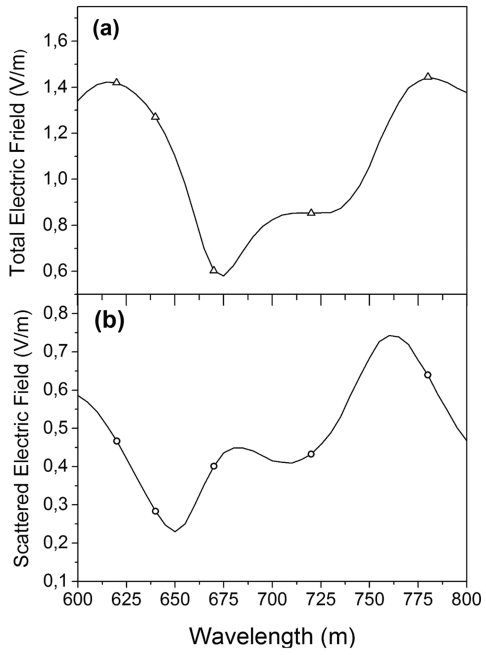

Figure 5. (a) Total and (b) scattered electric field in the middle point (near-field) of the considered nanostructure (d = 360 nm) as a function of the incident wavelength around that satisfying Kerker's conditions. Circles highlight the spectral position of the results shown in Figure 6.

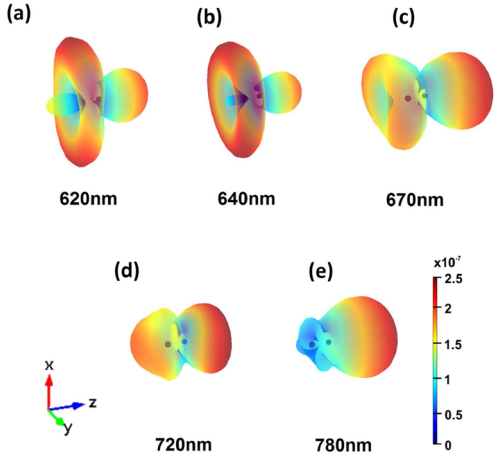

Figure 6. Spatial distribution of the scattered field of the optimum dimer in the far-field region for several incident wavelengths around that ones at which Kerker's conditions are satisfied for each nanoparticle. The interparticle distance is 360 nm.

Although previous simulations were carried out at 700 nm, this spectral analysis highlights that the fullfilment of Kerker's conditions is produced at 650 nm (global minimum at Figure 5b for the scattered field). The disagreement may be produced by the slight spectral shift of the resonances between the near- and the far-field region, as it was explained previously.[42] In addition, as before, the consideration of the total electric field produces a redshift of the minimum toward 675 nm. Nevertheless, it can be seen that a slight modulation of the incident wavelength (< 30 nm) could produce an important change in the electric field intensity in the gap region, in particular in the direction that is normal to the structure axis. In addition, a change of the wavelength smaller than 100 nm can

DOI: 10.1021/acs.jpcc.5b06302
J. Phys. Chem. C 2015, 119, 19558–19564

produce the switch from a minimum to a maximum field measured in the gap region. The measurement of the electric field in the near-field region is still a technological challenge that involves complex techniques.[43,44] For this reason, we are interested in the far-field distribution. Figure 6a−e show the scattered electric field distribution in the far field region of the considered nanostructure at certain wavelengths, corresponding with those highlighted in Figure 5. From the global minimum (λ = 670 nm), an increase of the wavelength produces a reinforcement of the scattering in the forward direction with respect to the backward direction. This produces a distribution of the scattered field that is focused on the forward direction, ocluding the increase of intensity in the central point at 780 nm. Under these conditions, it is not trivial to distinguish between the local minimum (720 nm, see Figure 5a) and the local maximum (780 nm) of the field in the gap region. On the other hand, if the incident wavelength is modulated such that it varies from the optimum wavelength to smaller values of λ (λ = 620 nm corresponds to a maximum, see Figure 5a), an important lobule, normal to the incident direction, emerges. In that case, a remarkable change in the far field region can be observed, and its measurement can be more viable, because the rest of the field still has relatively low values.

From an application point of view, the strong difference of the scattered field in the far field region and at a direction perpendicular to the axis of the dimer between two different, but close, incident wavelengths can be used to design an all-optical switch. As the signal at the considered wavelengths is not clearly larger than at the dipolar resonances, this system cannot be used as a nanoantenna. For that purpose, other works have already proposed alternative efficient nanostructures.[34,45] However, a switch is based here on a distinguishable variation of the signal such that it could be observed in our system. The small size of the system, their CMOS compatibility as well as the simplicity of the structure can be important advantages for a futuristic device for optical circuitry applications.

The same analysis can be extended to other semiconductor materials, as their electric and magnetic dipoles behave in a similar way, such that a proper combination of the two nanoparticles sizes, wavelength[40] and distance can be found. Figures 7a,b show the same information that Figure 5a,b for TiO_2 nanoparticles. Following the same process as in silicon, we consider two TiO_2 nanoparticles (R_1 = 78 nm and R_2 = 93 nm) satisfying Kerker's conditions at the same incident wavelength (λ = 543 nm) and separated a distance d = 235 nm. Parameters were optimized to obtain a minimum concentration of light in the middle point between nanoparticles at the wavelength satisfying Kerker's conditions. As it can be seen, a similar behavior of the silicon dimer is obtained, with the characteristic valley between two maximum. This result shows that a wide range of materials can be used, increasing the possible applications mentioned as a conclusion of the result above for silicon.

CONCLUSIONS

In this work, we explore the feasibility of designing an all-optical switch using the anisotropic scattering of semiconductor nanoparticles. In particular, we analyze a dimer composed of two silicon nanoparticles with sizes such that each one satisfies one of the Kerker's conditions at the same incident wavelength. Two opposite arrangements were considered and we observe the appearance of either a maximum or a minimum of the scattered field in the near field range, at the middle point between the particles and at a convenient wavelength. In addition, in the far-field region, we observe that the scattered radiation in the direction normal to the dimer axis also changes depending on the satisfaction of the Kerker's conditions. Due to the high dependence of Kerker's conditions on the incident wavelength, small shifts of the wavelength involve strong changes of the scattered radiation, both in the near- and far-field areas. Parameters, such as particle sizes, distance between the particles and the incident wavelength were numerically optimized in order to obtain a maximum contrast between the two states, satisfying or not Kerker's conditions. Due to the complex measurement of the scattered radiation, we also considered measurements of the total electric field, observing similar behaviors. In addition, these behaviors were confirmed using other semiconductor materials, as TiO_2, enlarging the design parameters.

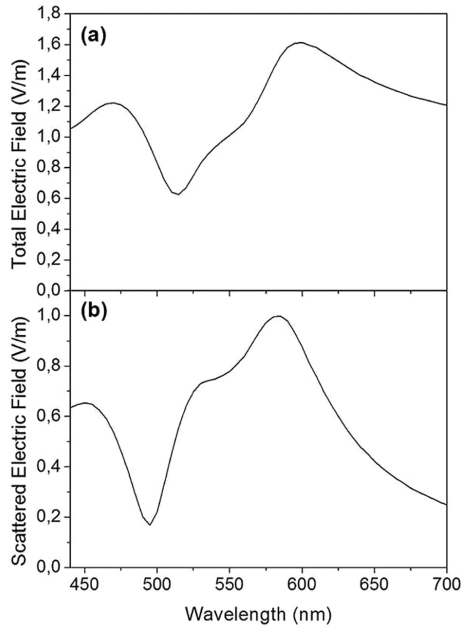

Figure 7. (a) Total and (b) scattered electric field in the middle point (near-field) of a nanostructure similar to that consider in Figure 4 composed TiO_2 nanospheres of sizes (R_1 = 78 nm and R_2 = 93 nm) and separated 235 nm as a function of the incident wavelength around that satisfying Kerker's conditions.

In spite of the small signal of the scattered radiation by these nanoparticles, disabling its use at nanoantennas, the important contrast between the considered states may be used as a switch parameter. The simplicity of the system, its dimensions, the CMOS compatibility of the materials, and the tunability of the operation wavelength using other materials and sizes are important aspects to take into account in the design of a futuristic integrated all-optic switch for computing applications.

AUTHOR INFORMATION

Corresponding Author

*Tel.: +34-916245964. E-mail: brgarcia@ing.uc3m.es.

Notes

The authors declare no competing financial interest.

ACKNOWLEDGMENTS

This work has been supported by Ministerio de Economía y Competitividad of Spain (Grant Nos. TEC2013−47342-C2−2-

DOI: 10.1021/acs.jpcc.5b06302
J. Phys. Chem. C 2015, 119, 19558−19564

R, TEC2012−38901-C02−01, and TEC2013−50138-EXP) and the R&D Program SINFOTON S2013/MIT-2790 of the Comunidad de Madrid.

REFERENCES

(1) Feynman, R. P. There's Plenty of Room at the Bottom. *Eng. Sci.* **1960**, *23*, 22−36.
(2) Sepúlveda, B.; Angelomè, P. C.; Lechuga, L.; Liz-Marzán, L. M. LSPR-Based Nanobiosensors. *Nano Today* **2009**, *4*, 244−251.
(3) Kuramochi, E.; Nozaki, K.; Shinya, A.; Takeda, K.; Sato, T.; Matsuo, S.; Taniyama, H.; Sumikura, H.; Notomi, M. Large-Scale Integration of Wavelength-Addressable All-Optical Memories on a Photonic Crystal Chip. *Nat. Photonics* **2014**, *8*, 474−481.
(4) Ahn, J.; Fiorentino, M.; Beausoleil, R. G.; Binkert, N.; Davis, A.; Fattal, D.; Jouppi, N. P.; McLaren, M.; Santori, C. M.; Schreiber, R. S.; et al. Devices and Architectures for Photonic Chip-Scale Integration. *Appl. Phys. A: Mater. Sci. Process.* **2009**, *95*, 989−997.
(5) Caulfield, H. J.; Dolev, S. Why Future Supercomputing Require Optics? *Nat. Photonics* **2010**, *4*, 261−263.
(6) Nicolas, A.; Veissier, L.; Giner, L.; Giacobino, E.; Maxein, D.; Laurat, J. A Quantum Memory for Orbital Angular Momentum Photonic Qubits. *Nat. Photonics* **2014**, *8*, 234−238.
(7) Lee, B. G.; Rylyakov, A. V.; Green, W. M. J.; Assefa, S.; Baks, C. W.; Rimolo-Donadio, R.; Kuchta, D. M.; Khater, M. H.; Barwicz, T.; Reinholm, C.; et al. Monolithic Silicon Integration of Scaled Photonic Switch Fabrics, CMOS Logic, and Device Driver Circuits. *J. Lightwave Technol.* **2014**, *32*, 743−751.
(8) García-Cámara, B. In *Communication Architectures for Systems-on-Chip*; Ayala, J. L., Ed.; CRC Press: Boca Raton, FL, 2011; pp 249−332.
(9) Taubenblatt, M. A. Optical Interconnects for High-Performance Computing. *J. Lightwave Technol.* **2012**, *30*, 448−457.
(10) Sihvola, A. Enabling Optical Analog Computing with Metamaterials. *Science* **2014**, *343*, 144−145.
(11) Vandoorne, K.; Mechet, P.; Van Vaerenbergh, T.; Fiers, M.; Morthier, G.; Verstraeten, D.; Schrauwen, B.; Dambre, J.; Bienstman, P. Experimental Demonstration of Reservoir Computing on a Silicon Photonic Chip. *Nat. Commun.* **2014**, *5*, 3541.
(12) Prasad, P. N. *Nanophotonics*; Wiley Interscience: New York, 2004.
(13) Maier, S. A. *Plasmonics: Fundamentals and Applications*; Springer: Berlin; Heidelberg, 2007.
(14) Homola, J. *Surface Plasmon Resonance based Sensors*; Springer: Berlin; Heidelberg, 2006.
(15) Algorri, J. F.; García-Cámara, B.; Urruchi, V.; Sánchez-Pena, J. M. High-Sensitivity Fabry-Perot Temperature Sensors based on Liquid Crystal Doped with Nanoparticles. *IEEE Photonics Technol. Lett.* **2015**, *27*, 292−295.
(16) Cuadrado, A.; Briones, E.; González, F. J.; Alda, J. Polarimetric Pixel using Seebeck Nanoantenna. *Opt. Express* **2014**, *22*, 13835−13845.
(17) Wu, L.; Reinhard, B. M. Probing Subdiffraction Limit Separations with Plasmon Coupling Microscopy: Concepts and Applications. *Chem. Soc. Rev.* **2014**, *43*, 3884−3897.
(18) Novotny, L.; van Hulst, N. Antennas for Light. *Nat. Photonics* **2011**, *5*, 83−90.
(19) Cuadrado, A.; Alda, J.; González, F. J. Distributed Bolometric Effect in Optical Antennas and Resonant Structures. *J. Nanophotonics* **2012**, *6*, 1−10.
(20) García-Etxarri, A.; Gómez-Medina, R.; Froufe-Pérez, L. S.; López, C.; Chantada, L.; Scheffold, F.; Aizpurua, J.; Nieto-Vesperinas, M.; Sáenz, J. J. Strong Magnetic Response of Submicron Silicon Particles in the Infrared. *Opt. Express* **2011**, *19*, 4815−4826.
(21) Gómez-Medina, R.; García-Cámara, B.; Súarez-Lacalle, I.; González, F.; Moreno, F.; Nieto-Vesperinas, M.; Sáenz, J. J. Electric and Magnetic Dipolar Response of Germanium Nanospheres: Interference Effects, Scattering Anisotropy, and Optical Forces. *J. Nanophotonics* **2011**, *5*, 053512.
(22) Krasnok, A.; Makarov, S.; Petrov, M.; Savelev, R.; Belov, P.; Kivshar, Y. Towards All-Dielectric Metamaterials and Nanophotonics. *arXiv*:**2015***1503*, 08857 [physics.optics].10.1117/12.2176880
(23) Zheludev, N. I. The Road Ahead for Metamaterials. *Science* **2010**, *328*, 582−583.
(24) Maas, R.; Parsons, J.; Engheta, N.; Polman, A. *Experimental Realization of an Epsilon-Near-Zero Metamaterials at Visible Wavelengths*. *Nat. Photonics* **2013**, *7*, 907−912.
(25) Moitra, P.; Yang, Y.; Anderson, Z.; Kravchenko, I. I.; Briggs, D. P.; Valentine, J. Realization of an All-Dielectric Zero-Index Optical Metamaterial. *Nat. Photonics* **2013**, *7*, 791−795.
(26) Giannini, V.; Fernández-Dominguez, A. I.; Heck, S. C.; Maier, S. A. Plasmonic Nanoantennas: Fundamentals and Their Use in Controlling the Radiative Properties of Nanoemitters. *Chem. Rev.* **2011**, *111*, 3888−3912.
(27) Krasnok, A. E.; Simovski, C. R.; Belov, P. A.; Kivshar, Y. S. Superdirective Dielectric Nanoantennas. *Nanoscale* **2014**, *6*, 7354−7361.
(28) Fano, U. Effects of Configuration Interaction on Intensities and Phase Shifts. *Phys. Rev.* **1961**, *124*, 1866.
(29) Luk'yanchuk, B.; Zheludev, N. I.; Maier, S. A.; Halas, N. J.; Norlander, P.; Giessen, H.; Chong, C. T. The Fano Resonance in Plasmonic Nanostructures and Metamaterials. *Nat. Mater.* **2010**, *9*, 707−715.
(30) Miroshnichenko, A. E.; Kivshar, Y. S. Fano Resonance in All-Dielectric Oligomers. *Nano Lett.* **2012**, *12*, 6459−6463.
(31) Kuznetsov, A. I.; Miroshnichenko, A. E.; Fu, Y. H.; Zhang, J. B.; Luk'yanchuk, B. Magnetic Light. *Sci. Rep.* **2012**, *2*, 492.
(32) Cai, D.-J.; Huang, Y.-H.; Wang, W.-J.; Ji, W.-B.; Chen, J.-D.; Chen, Z.-H.; Liu, S.-D. Fano Resonances Generated in a Single Dielectric Homogeneous Nanoparticle with High Structural Symmetry. *J. Phys. Chem. C* **2015**, *119*, 4252−4260.
(33) Chong, K. E.; Hopkins, B.; Staude, I.; Miroshnichenko, A. E.; Dominguez, J.; Decker, M.; Neshev, D. N.; Brener, I.; Kivshar, Y. S. Observation of Fano Resonances in All-Dielectric Nanoparticle Oligomers. *Small* **2014**, *10*, 1985−1990.
(34) Bakker, R. M.; Permyakov, D.; Yu, Y. F.; Markovich, D.; Paniagua-Domínguez, R.; Gonzaga, L.; Samusev, A.; Kivshar, Y.; Luk'yanchuk, B.; Kuznetsov, A. I. Magnetic and Electric Hotspots with Silicon Nanodimers. *Nano Lett.* **2015**, *15*, 2137−2142.
(35) Staude, I.; Miroshnichenko, A. E.; Decker, M.; Fofang, N. T.; Liu, S.; Gonzales, E.; Dominguez, J.; Luk, T. S.; Neshev, D. N.; Brener, I.; Kivsnar, Y. Tailong Directional Scattering through Magnetic and Electric Resonances in Subwavelength Silicon Nanodisks. *ACS Nano* **2013**, *7*, 7824−7832.
(36) Albella, P.; Poyli, M. A.; Schmidt, M. K.; Maier, S. A.; Moreno, F.; Sáenz, J. J.; Aizpurua, J. Low-Loss Electric and Magnetic Field-Enhanced Spectroscopy with Subwavelength Silicon Dimers. *J. Phys. Chem. C* **2013**, *117*, 13573−13584.
(37) Kerker, M.; Wang, D. S.; Giles, C. L. Electromagnetic Scattering by Magnetic Spheres. *J. Opt. Soc. Am.* **1983**, *73*, 765−767.
(38) Geffrin, J. M.; García-Cámara, B.; Gómez- Medina, R.; Albella, P.; Froufe-Pérez, L. S.; Eyraud, C.; Litman, A.; Vaillon, R.; González, F.; Nieto-Vesperinas, M.; Sáenz, J. J.; Moreno, F. Magnetic and Electric Coherence in Forward-and Back-Scattered Electromagnetic Waves by a Single Dielectric Subwavelength Sphere. *Nat. Commun.* **2012**, *3*, 1171.
(39) Bohren, C. F.; Huffman, D. R. *Absorption and Scattering of Light by Small Particles*; John Wiley & Sons: New York, 1983.
(40) Garcia-Cámara, B.; Algorri, J. F.; Cuadrado, A.; Urruchi, V.; Sánchez-Pena, J. M.; Vergaz, R. Size Dependence of the Directional Scattering Conditions on Semiconductor Nanoparticles. *IEEE Photonics Technol. Lett.* **2015**, 1.
(41) Lukyanchuk, B. S.; Voshchinnikov, N. V.; Paniagua-Dominguez, R.; Kuznetsov, A. I. Optimum Forward Light Scattering by Spherical and Spheroidal Dielectric Nanoparticles with High Refractive Index. *ACS Photonics* **2015**, *2*, 993−999.

DOI: 10.1021/acs.jpcc.5b06302
J. Phys. Chem. C 2015, 119, 19558−19564

(42) Moreno, F.; Albella, P.; Nieto-Vesperinas, M. Analysis of the Spectral Behavior of Localized Plasmon Resonances in the Near- and Far-Field Regimes. *Langmuir* **2013**, *29*, 6715−6721.
(43) Barnard, E. S.; Pala, R. A.; Brongersma, M. L. Photocurrent Mapping of Near-Field Optical Antenna Resonances. *Nat. Nanotechnol.* **2011**, *6*, 588−593.
(44) Volpe, G.; Noack, M.; Aćimović, S. S.; Reinhardt, C.; Quidant, R. Near-Field Mapping of Plasmonic Antennas by Multiphoton Absorption in Poly(Methyl Methacrylate). *Nano Lett.* **2012**, *12*, 4864−4868.
(45) Zywietz, U.; Schmidt, M. K.; Evlyukhin, A. B.; Reinhardt, C.; Aizpurua, J.; Chichkov, B. N. Electromagnetic Resonances of Silicon Nanoparticle Dimers in the Visible. *ACS Photonics* **2015**, *2*, 913−920.

DOI: 10.1021/acs.jpcc.5b06302
J. Phys. Chem. C 2015, 119, 19558−19564